

MSSM vs. NMSSM in $\Delta F = 2$ transitions

Jacky Kumar*

*Department of High Energy Physics, Tata Institute of Fundamental Research,
400 005, Mumbai, India*

E-mail: jka@tifr.res.in

We study deviations between MSSM and NMSSM in the predictions of $\Delta F = 2$ processes. We found that there can be two sources which can cause such deviations, i.e due to certain neutralino-gluino crossed box diagrams and due to well known double penguin diagrams. Both are effective at large $\tan\beta$. In addition to this, taking into account 8 TeV direct search constraints from the heavy Higgs searches, we study the maximum allowed MFV like new physics(NP) effects on ΔM_s in the two models. In NMSSM such NP effects can be as large as 25%, on the other hand in MSSM such large contributions are severely constrained.

*9th International Workshop on the CKM Unitarity Triangle
28 November - 3 December 2016
Tata Institute for Fundamental Research (TIFR), Mumbai, India*

*Speaker.

1. Setup

The next-to-minimal supersymmetric standard model (NMSSM) [1, 2] is known for providing a solution to the μ -problem[3] and accommodating a 125 GeV SM-like Higgs boson with relatively lesser fine tuning as compare to MSSM[4]. In addition to two Higgs doublets in MSSM, it contains an extra gauge singlet chiral superfield(S). The superpotential of Z_3 -invariant NMSSM is given by,

$$\mathcal{W} = \lambda H_u \cdot H_d S + \frac{\kappa}{3} S^3 + \mathcal{W}_{Yukawa}. \quad (1.1)$$

Where \mathcal{W}_{Yukawa} contains the Yukawa terms and λ, κ are the dimensionless couplings. NMSSM has an extended Higgs and neutralino sectors as compare to MSSM. For example the physical neutralino states are mixtures of gaugino, Higgsino and 'singlino' - the fermion component of the superfield S , weak eigen states. Although the stop sector, which has an additional source of quark flavor violation in supersymmetry(SUSY), remains unchanged. But there can still be additional effects of NMSSM on the quark flavor transitions due its modified neutralino and Higgs sectors. In this regard we study the $\Delta F = 2$ transitions in MSSM and NMSSM and address the following two questions,

- Can NMSSM, without any assumption on squark flavor structure, give different theoretical predictions for the $\Delta F = 2$ observables as compare to MSSM?. If so, what is the mechanism behind this.
- What are the largest allowed minimal flavor violating(MFV) effects[7] in MSSM and NMSSM in $\Delta F = 2$ observables at low $\tan\beta$?

First, we isolate all possible genuine NMSSM contributions(non-MSSM) to $\Delta F = 2$ transitions and figure out the conditions in which these two models give different predictions. The amplitude for $B - \bar{B}$ mixing is defined as $M_{12}^q = \langle B_q | H_{eff} | \bar{B}_q \rangle$, where $q = d, s$ stand for B_d, B_s mixing, respectively. The effective Hamiltonian, H_{eff} , can be consistently expressed in the basis of eight dimension-six operators Q_i as,

$$H_{eff} = \sum_i C_i Q_i + h.c, \quad (1.2)$$

with C_i being their respective Wilson Coefficients (WC). We follow the operator basis defined in [6], which reads explicitly,

$$Q^{VLL} = (\bar{b}_L \gamma_\mu q_L)(\bar{b}_L \gamma^\mu q_L), \quad Q^{VLR} = (\bar{b}_L \gamma_\mu q_L)(\bar{b}_R \gamma^\mu q_R), \quad Q^{SLR} = (\bar{b}_R q_L)(\bar{b}_L q_R), \quad (1.3)$$

$$Q_1^{SLL} = (\bar{b}_R q_L)(\bar{b}_R q_L), \quad Q_2^{SLL} = (\bar{b}_R \sigma_{\mu\nu} q_L)(\bar{b}_R \sigma^{\mu\nu} q_L). \quad (1.4)$$

In the above expressions, the diagonal quark-color indices are suppressed (assumed to be contracted separately within each bracket), and $\sigma_{\mu\nu} = \frac{1}{2}[\gamma_\mu, \gamma_\nu]$. The remaining three operators, $Q^{VRR}, Q_1^{SRR}, Q_2^{SRR}$ are obtained from $Q^{VLL}, Q_1^{SLL}, Q_2^{SLL}$ by interchanging L with R . In SM only Q^{VLL} gets non-zero contribution from one-loop *box diagrams* with quarks and W -bosons circulating in the loops. But in MSSM there are various, additional, box contributions mediated by: 1) charged Higgs, up-quarks; 2) chargino, up-squarks; 3) gluinos, down-squarks; 4) neutralinos, down-squarks; 5) gluino, neutralino, down squarks [5]. Their diagrammatic topologies are shown in Fig.1. Certain two-loop diagrams (*i.e.*, *double-penguins*) which depend on positive powers of $\tan\beta$ become also relevant for large values of this parameter and can easily dominate over any other contribution [6].

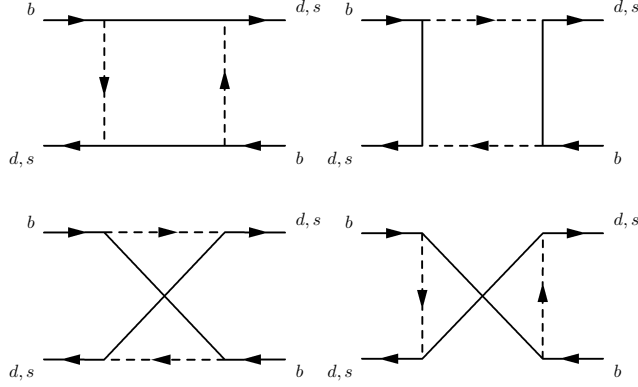


Figure 1: One-loop box diagrams contributing to $\Delta F = 2$ observables.

1.1 NMSSM contributions to ΔM_s

There can be two kind of genuine NMSSM effects, 1) due to presence of an extra neutralino state 2) due to additional Higgs bosons. The extra neutralino state trivially affects the neutralino-quark-squark vertex(V), which appears in the box diagrams shown in Fig.1. But this can leave strong imprints on the observables. However we find that the largest new effects arise only due to the crossed box diagrams mediated by neutralino and gluino. A typical WC originating from neutralino-gluino contributions in the mass basis has a form (see Appendix A of [8] for all WCs),

$$C_1^{SRR} = \frac{g_3^2}{16\pi^2} \frac{7}{6} V_{2ka}^R V_{3la}^{L*} Z_{3k}^* Z_{5l} m_{\tilde{g}} m_a D_0(m_{\tilde{g}}^2, m_a^2, m_k^2, m_l^2) \\ + \frac{g_3^2}{16\pi^2} \frac{1}{6} (V_{3ka}^{L*} V_{3la}^{L*} Z_{5k} Z_{5l} + V_{2ka}^R V_{2la}^R Z_{3k}^* Z_{3l}^*) m_{\tilde{g}} m_a D_0(m_{\tilde{g}}^2, m_a^2, m_k^2, m_l^2). \quad (1.5)$$

Since singlino mixes only with the Higgsino's via first term in the superpotential Eq(1.1), so keeping only Yukawa related terms in the vertex (V), we identify two types basic structures appearing in all the WCs,

$$m_{\tilde{g}} (Z_N)_{3a} m_a D_0(m_{\tilde{g}}^2, m_a^2, x) (Z_N)_{3a} \quad (1.6)$$

$$(Z_N)_{3a} D_2(m_{\tilde{g}}^2, m_a^2, x) (Z_N)_{3a}^* \quad (1.7)$$

where the other factors like $g_3^2 Y_b^2$, Z_D are suppressed and the two down-squark mass arguments of the loop-functions are suppressed into the argument x . Up to complex conjugation in the above expressions, one can easily verify that there is no other structure [9].

Next, to isolate the genuine NMSSM contributions, we use (Flavor expansion theorem)FET[9], and translate the mass eigen state expressions of Eq(1.5) into the Mass Insertion Approximation(MIA) expansion, i.e.

$$m_{\tilde{g}} \left[\mathbf{M}_N D_0(m_{\tilde{g}}^2, \mathbf{M}_N^2, x) \right]_{33} = m_{\tilde{g}} (M_N)_{35} (M_N^2)_{53} E_0(m_{\tilde{g}}^2, (M_N^2)_{55}, (M_N^2)_{33}, x) + \dots \quad (1.8)$$

$$\left[D_2(m_{\tilde{g}}^2, \mathbf{M}_N^2, x) \right]_{33} = D_2(m_{\tilde{g}}^2, (M_N^2)_{33}, x) + \dots \quad (1.9)$$

where the dots represent the terms higher order in the neutralino mass insertions(higher order in FET). The explicit form of all loop functions D_0 , D_2 and E_0 can be found in [8]. The leading

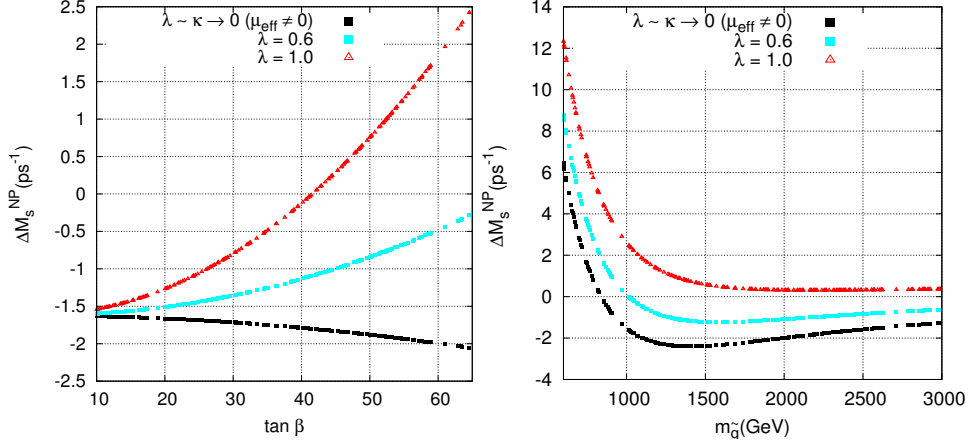


Figure 2: Genuine-NMSSM effects in ΔM_s , understood as deviations with respect to the MSSM predictions under $\tan\beta$ (left) and gluino mass (right), scaling. Input parameters primarily controlling the effect read $(m_D^2)_{ii} = 650 \text{ GeV}$, $M_S = 3 \text{ TeV}$, $\delta_{RR}^{23} = 0.6$, while $m_{\tilde{g}} = 1.1 \text{ TeV}$ and $\tan\beta = 60$ were used for left and right plot, respectively. Cyan line ($\kappa = 0.4$) corresponds to perturbative NMSSM up to GUT-scale. Red line ($\kappa = 1$) requires UV-completion before GUT-scale, as in λ -SUSY models. The black line is the MSSM-limit of the NMSSM model. For other parameters see text. Calculations are performed in mass basis taking into account all contributions.

genuine-NMSSM effects come from E_0 -terms, having a strong dependence on λ, κ -parameters through neutralino mass matrix elements $(M_N)_{35}$ and $(M_N^2)_{53}$ which are, in addition, related to ν_u . Although suppressed by a neutralino mass insertion these can be important when Higgsino-singlino, i.e. $\tilde{H}_d^0 - \tilde{S}$ mixing is sufficiently large. The D_2 -terms are less sensitive to the NMSSM parameters λ, κ since these appear only through the $(M_N^2)_{33}$ argument of the respective loop function. In this sense, D_2 -terms mediate *mixed effects* which is understood by the fact that they are non-zero in the MSSM limit, $\lambda \sim \kappa \rightarrow 0$. Typically, the E_0 -terms are safe from D_2 -term screening, since they are primarily associated with different types of squark mass insertions. Nevertheless, due to neutralino mass insertion suppression, the E_0 -term can become comparable to other neutralino-gluino MSSM contributions. These are sub-leading in the couplings (e.g., $\propto Y_b Y_s, g_2^2$, etc.) but not suppressed by neutralino insertions. In Fig.2, we present the relative magnitude of genuine-NMSSM and MSSM contributions. Left panel shows ΔM_s as a function of $\tan\beta$, while right plot shows the variation of same with gluino mass. The qualitative analysis above dictates following general properties of NMSSM enhanced region. Large values of $\tan\beta$ and $\lambda \sim \kappa$ are required. The former condition enhances the down-type Yukawa couplings which are present in \tilde{H}_d^0 interactions. The latter condition is required for large Higgsino-singlino mixing which controls the size of genuine-NMSSM contributions. Typical values for significant effects are $50 \lesssim \tan\beta \lesssim 65$ and $0.5 \lesssim \kappa \sim \lambda \lesssim 1$. Large values of M_A are preferable, which suppress both charged Higgs contributions and double penguins effects. This is also motivated by the Higgs potential in the large $\tan\beta, \lambda$ regime of NMSSM, as discussed in appendix C of [8]. There, we display the method of obtaining phenomenologically viable CP-even and CP-odd scalar masses by fitting the soft A_λ, A_κ parameters, while keeping λ, κ as free parameters. The typical range for M_A obtained this way is $4 \text{ TeV} \lesssim M_A \lesssim 12 \text{ TeV}$, depending on $\mu_{eff}, \tan\beta$ inputs.

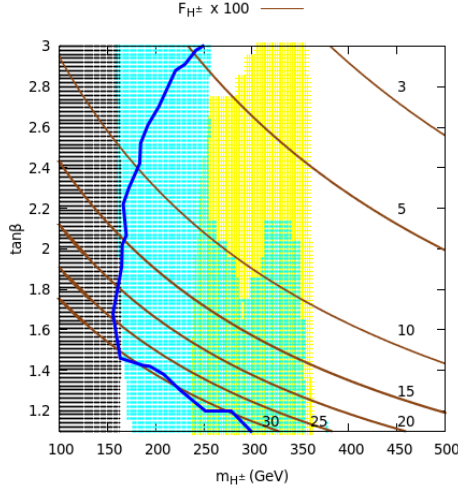


Figure 3: Brown contours shows percentage modification F_{H^\pm} to $\Delta F = 2$ observables involving charged Higgs. Gray ($H^+ \rightarrow \tau^+ \nu$), cyan ($H \rightarrow ZZ$) and yellow ($A \rightarrow hZ$) regions are hMSSM exclusions at 95%CL. NMSSM exclusion is on the left-side of the blue contour.

Another source of genuine NMSSM effects is double penguin diagrams. The situation in this case is more involved and although the effect of an extra neutralino circulating in loops is in practice irrelevant, the extra CP-even and CP-odd singlet states induce various modifications in relevant couplings and spectra. NMSSM effects in double penguin diagrams are effective mostly when mass of lighter pseudoscalar is around 5 GeV (which is the B-meson mass). This is basically a resonance effect. This effect can cause even an order of magnitude enhanced NP contributions at the resonance and is effective only at large $\tan\beta$ [8].

1.2 Upper bounds on new physics in $\Delta F = 2$ for MFV models at $\tan\beta$ in MSSM and NMSSM

From our previous analysis we conclude that at low $\tan\beta$ NMSSM gives same predictions for $\Delta F = 2$ transitions irrespective of MFV assumption. It is to be noted that common SUSY-parameter of both models has to lie in physical parameter space. After Higgs discovery MSSM at low $\tan\beta$ survives only through hMSSM scenario[10], which requires a very high SUSY scale to reach to 125 GeV Higgs mass at low $\tan\beta$. It is known that with the MFV assumption once we take into account the direct search bounds on sparticles, the dominant contribution comes from charged Higgs diagrams[11]. This simplifies the picture a lot, because charged Higgs contributions are mainly controlled by two parameters M_A and $\tan\beta$. On the other hand direct searches at the LHC has set stringent bounds on the these two parameter. Particularly the searches sensitive to low $\tan\beta$ include $H \rightarrow ZZ$ [12], $H^+ \rightarrow \tau\nu$ [14], $A \rightarrow hZ$ [13]. We employ 8TeV data in these channels to set limits on the charged Higgs mass as a function of $\tan\beta$ in both the models. Using these limits we set upper bound on NP in $\Delta F = 2$ observables. This is shown in Fig. 3. The brown contours represent the percentage deviations F_{H^\pm} in $\Delta F = 2$ due to charged Higgs contribution. Clearly $O(25)\%$ contribution is MSSM is severely constrained, on the other hand in NMSSM the situation is more relaxed. This means for NMSSM, at present constraints on the $M_A - \tan\beta$ plane coming from flavor physics sector are comparable or stronger than direct searches.

2. Summary

We study genuine NMSSM contributions to $\Delta F = 2$ transitions. We find that such effects can come either from certain neutralino-gluino crossed box diagram, due to the extended neutralino sector of NMSSM, and from double-penguin diagrams due to the extra scalar states, both are effective in the large $\tan\beta$ regime. We also study the low $\tan\beta$ regime, where a distinction between these two models in $\Delta F = 2$ processes can come indirectly, due to different constraints on the allowed parameter space of the two models. To this end, we incorporate the recent limits from $H \rightarrow ZZ$, $A \rightarrow hZ$ and $H^\pm \rightarrow \tau\nu$ along with Higgs observables and set upper bounds on the new physics contributions of the two models under the MFV assumption. We find that an $O(25\%)$ contribution in $\Delta F = 2$, originating from charged-Higgs diagrams is still possible in both models, however such a large effect is severely constrained in the case of MSSM due to stronger bounds on the charged Higgs mass.

Acknowledgements: I would like to thank the organizers of CKM 2016 workshop for giving an opportunity to present this work. Also, thanks to Michael paraskevas for a pleasant collaboration in this work.

References

- [1] P. Fayet, Nucl. Phys. B **90**, 104 (1975). doi:10.1016/0550-3213(75)90636-7
- [2] U. Ellwanger, C. Hugonie and A. M. Teixeira, Phys. Rept. **496**, 1 (2010) doi:10.1016/j.physrep.2010.07.001 [arXiv:0910.1785 [hep-ph]].
- [3] J. E. Kim and H. P. Nilles, Phys. Lett. **138B**, 150 (1984). doi:10.1016/0370-2693(84)91890-2
- [4] L. J. Hall, D. Pinner and J. T. Ruderman, JHEP **1204**, 131 (2012) doi:10.1007/JHEP04(2012)131 [arXiv:1112.2703 [hep-ph]].
- [5] W. Altmannshofer, A. J. Buras and D. Guadagnoli, JHEP **0711**, 065 (2007) doi:10.1088/1126-6708/2007/11/065 [hep-ph/0703200].
- [6] A. J. Buras, P. H. Chankowski, J. Rosiek and L. Slawianowska, Nucl. Phys. B **659**, 3 (2003) doi:10.1016/S0550-3213(03)00190-1 [hep-ph/0210145].
- [7] G. D'Ambrosio, G. F. Giudice, G. Isidori and A. Strumia, Nucl. Phys. B **645**, 155 (2002) doi:10.1016/S0550-3213(02)00836-2 [hep-ph/0207036].
- [8] J. Kumar and M. Paraskevas, JHEP **1610**, 134 (2016) doi:10.1007/JHEP10(2016)134 [arXiv:1608.08794 [hep-ph]].
- [9] A. Dedes, M. Paraskevas, J. Rosiek, K. Suxho and K. Tamvakis, JHEP **1506**, 151 (2015) doi:10.1007/JHEP06(2015)151 [arXiv:1504.00960 [hep-ph]].
- [10] A. Djouadi, L. Maiani, G. Moreau, A. Polosa, J. Quevillon and V. Riquer, Eur. Phys. J. C **73**, 2650 (2013) doi:10.1140/epjc/s10052-013-2650-0 [arXiv:1307.5205 [hep-ph]].
- [11] R. Barbieri, D. Buttazzo, F. Sala and D. M. Straub, JHEP **1405**, 105 (2014) doi:10.1007/JHEP05(2014)105 [arXiv:1402.6677 [hep-ph]].
- [12] The ATLAS collaboration [ATLAS Collaboration], ATLAS-CONF-2016-082.
- [13] The ATLAS collaboration, ATLAS-CONF-2016-015.

- [14] M. Aaboud *et al.* [ATLAS Collaboration], Phys. Lett. B **759**, 555 (2016)
doi:10.1016/j.physletb.2016.06.017 [arXiv:1603.09203 [hep-ex]].